

# Singularity-Invariant Families of Line-Plane 5-SPU Platforms

Júlia Borràs, Federico Thomas and Carme Torras

**Abstract**— A 5-SPU robot with collinear universal joints is well suited to handling an axisymmetric tool, since it has 5 controllable DoFs and the remaining one is a free rotation around the tool. The kinematics of such a robot having also coplanar spherical joints has previously been studied as a rigid subassembly of a Stewart-Gough platform, it being denoted a line-plane component. Here we investigate how to move the leg attachments in the base and the platform without altering the robot’s singularity locus. By introducing the so-called 3D space of leg attachments, we prove that there are only three general topologies for the singularity locus corresponding to the families of quartically-, cubically- and quadratically-solvable 5-SPU robots. The members of the last family have only 4 assembly modes, which are obtained by solving two quadratic equations. Two practical features of these quadratically-solvable robots are the large manipulability within each connected component and the fact that, for a fixed orientation of the tool, the singularity locus reduces to a plane.

**Index Terms**— Parallel manipulators, Gough-Stewart platforms, robot kinematics, kinematics singularities, manipulator design.

## I. INTRODUCTION

Over the past half-century, the Stewart-Gough platform has been applied extensively to automate many different tasks due to its well-known merits in terms of speed, rigidity, dynamic bandwidth, accuracy, cost, etc. [1], [2]. There are many important industrial tasks requiring a tool to be perpendicular to a 3D free-from surface along a given trajectory. They include 5-axis milling, laser-engraving, spray-based painting, water-jet cutting, and, in general, any manipulation task in which the tool is axisymmetric. These tasks can be performed by robots with only 3 translations and 2 rotations; *i.e.*, 5 DoF (degrees of freedom). Since the Stewart-Gough platform has 6 DoF, some limited-DoF parallel robots have been designed for this kind of applications with the aim of simplifying the structure and the control of the general Stewart-Gough platform but without losing its aforementioned merits [3], [4], [5], [6], [7].

The Stewart-Gough platform consists of a base and a moving platform connected by six UPS (Universal-Prismatic-Spherical) legs, where the underline indicates that the prismatic joint is actuated. Thus, it is usually referenced to as a 6-UPS, or equivalently as a 6-SPU, parallel mechanism. If

The authors are with the Institut de Robòtica i Informàtica Industrial (CSIC-UPC), Llorens Artigas 4-6, 08028 Barcelona, Spain. E-mails: {jborras, fthomas, ctorras}@iri.upc.edu

This work has been partially supported by the Generalitat de Catalunya through the Robotics group and ACCIÓ. The paper has supplementary downloadable material provided by the authors, which includes a video of a functioning 5-SPU prototype, a video illustrating its underlying geometry, MAPLE worksheets together with webpage explanations for examples of 5-SPU robots with quartic, cubic and quadratic forward kinematics solutions, as well as for the redesign example in Section III-D. The material is 10 MB in size.

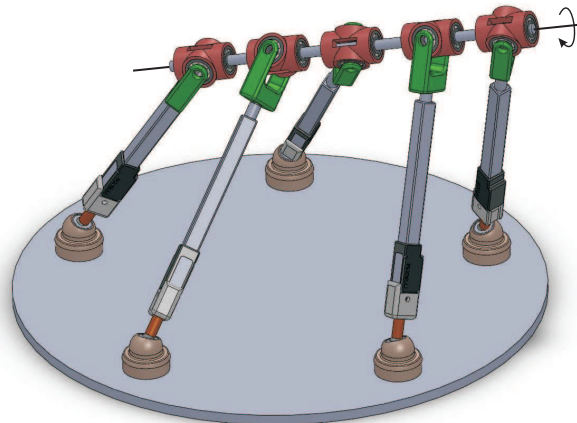


Fig. 1. A 5-SPU parallel robot with aligned universal joints. While the axis defined by these universal joints is rigidly linked to the base for fixed leg lengths, any tool attached to it can freely rotate.

one of these legs is eliminated to obtain a 5-DoF parallel robot, two alternatives arise to make the moving platform location controllable; namely: (1) adding an extra passive leg, or (2) restraining the mobility of one of the five remaining legs. Then, the challenge consists in how to perform any of these two operations so that the resulting robot has 3 translations and 2 rotations. Y. Zhao and colleagues beat the challenge for the first alternative. They proposed to introduce a PRPU (Prismatic-Revolute-Prismatic-Revolute) passive leg. The properties of the resulting mechanism, technically referenced to as a 5-UPS+PRPU mechanism for obvious reasons, has been analyzed in a series of papers [8], [9], [10]. More recently, Y. Lu and colleagues opted for the second alternative. They proposed a 4-UPS+SPR parallel platform whose static and dynamic properties are studied in [11] and [12], respectively. Many other examples of 5-DoF parallel robots can be found in literature but they greatly depart from the basic 6-UPS design in the sense that they do not contain at least 4 UPS legs.

A parallel robot consisting of a base and a moving platform connected by five SPU legs is clearly uncontrollable. For example, if the universal joints are aligned as in Fig. 1, the moving platform can freely rotate around the axis defined by the five aligned revolute joints. If this rotation axis is made coincident with the symmetry axis of the tool, the uncontrolled motion becomes irrelevant in most cases, and the 5 leg actuators control the remaining 5 degrees of freedom. Alternatively, this uncontrolled motion can always be eliminated by blocking one of the five aligned revolute joints. The presented analysis is valid irrespective of this choice. Kong and Gosselin refer to the



which depends exclusively on the 5-legged 5-DoF component.

Thus, the singularity locus of the 5-S $\underline{\text{P}}\underline{\text{U}}$  manipulator studied in this paper corresponds to the root locus of the polynomial resulting from expanding such determinant, i.e.,

$$C_1 w p_z + C_2 w (p_z u - p_x w) + C_3 w (p_z v - p_y w) + C_4 p_z (p_x w - p_z u) + C_5 p_z (p_y w - p_z v) - C_6 w^2 = 0, \quad (2)$$

where  $C_i$ , for  $i = 1, \dots, 6$ , is the cofactor of the  $(1, i)$  entry of  $\mathbf{T}$ , which depends only on leg attachments. In what follows, we assume that not all  $C_i$  are equal to zero, since in this case  $\det(\mathbf{T})$  would be identically zero irrespective of the pose of the platform, which would thus be architecturally singular.

### B. Forward Kinematics

Similarly to [16], the forward kinematics of our 5-legged parallel robot can be solved by writing the leg lengths as  $l_i = \|\mathbf{b}_i - \mathbf{a}_i\|$ , for  $i = 1, \dots, 5$ . Then, subtracting from the expression for  $l_i^2$ ,  $i = 1, \dots, 5$ , the equation  $\|\mathbf{i}\| = u^2 + v^2 + w^2 = 1$ , quadratic terms in  $u$ ,  $v$  and  $w$  cancel out yielding

$$z_i t - x_i p_x - y_i p_y - x_i z_i u - y_i z_i v + \frac{1}{2}(p_x^2 + p_y^2 + p_z^2 + x_i^2 + y_i^2 + z_i^2 - l_i^2) = 0, \quad (3)$$

for  $i = 1, \dots, 5$ , where  $t = \mathbf{p} \cdot \mathbf{i}$ .

Subtracting the first equation from the others, quadratic terms in  $p_x$ ,  $p_y$  and  $p_z$  cancel out as well. Then, the resulting system of equations can be written in matrix form as

$$\begin{pmatrix} x_2 - x_1 & y_2 - y_1 & x_2 z_2 - x_1 z_1 & y_2 z_2 - y_1 z_1 \\ x_3 - x_1 & y_3 - y_1 & x_3 z_3 - x_1 z_1 & y_3 z_3 - y_1 z_1 \\ x_4 - x_1 & y_4 - y_1 & x_4 z_4 - x_1 z_1 & y_4 z_4 - y_1 z_1 \\ x_5 - x_1 & y_5 - y_1 & x_5 z_5 - x_1 z_1 & y_5 z_5 - y_1 z_1 \end{pmatrix} \begin{pmatrix} p_x \\ p_y \\ u \\ v \end{pmatrix} = \begin{pmatrix} (z_2 - z_1)t + N_2 \\ (z_3 - z_1)t + N_3 \\ (z_4 - z_1)t + N_4 \\ (z_5 - z_1)t + N_5 \end{pmatrix}, \quad (4)$$

where

$$N_i = \frac{1}{2}(x_i^2 + y_i^2 + z_i^2 - l_i^2 - x_1^2 - y_1^2 - z_1^2 + l_1^2). \quad (5)$$

Now, notice that the determinant associated with the linear system (4) can be written as

$$\begin{vmatrix} x_1 & y_1 & x_1 z_1 & y_1 z_1 & 1 \\ x_2 & y_2 & x_2 z_2 & y_2 z_2 & 1 \\ x_3 & y_3 & x_3 z_3 & y_3 z_3 & 1 \\ x_4 & y_4 & x_4 z_4 & y_4 z_4 & 1 \\ x_5 & y_5 & x_5 z_5 & y_5 z_5 & 1 \end{vmatrix}, \quad (6)$$

which coincides with  $C_1$  in (2). If (6) vanishes, either  $p_x$ ,  $p_y$ ,  $u$ , or  $v$ , can be chosen as parameter, instead of  $t$ , to reformulate the linear system (4). Since for a non-architecturally singular robot not all cofactors are zero, it can be shown that a non-singular linear system of the form (4) can always be found by choosing either  $t$ ,  $p_x$ ,  $p_y$ ,  $u$ , or  $v$  as parameter.

Solving (4) by Cramer's rule, and applying the multilinearity property of determinants, yields

$$\begin{aligned} p_x &= (-C_2 t + E_2)/C_1, \\ p_y &= (-C_3 t + E_3)/C_1, \\ u &= (-C_4 t + E_4)/C_1, \\ v &= (-C_5 t + E_5)/C_1, \end{aligned} \quad (7)$$

where  $E_i$  results from substituting the  $(i - 1)$ th column vector of the matrix in the system (4) by  $(N_2, \dots, N_5)^T$  and computing its determinant.

From equation  $u^2 + v^2 + w^2 = 1$  and equation (3) for  $i = 1$ , it can be concluded that:

$$\begin{aligned} p_z^2 w^2 &= (1 - u^2 - v^2) \\ [2(-z_1 t + x_1 p_x + y_1 p_y + z_1 y_1 v + z_1 x_1 u) \\ - p_x^2 - p_y^2 - x_1^2 - y_1^2 - z_1^2] &. \end{aligned} \quad (8)$$

One the other hand, from  $t = \mathbf{p} \cdot \mathbf{i}$ ,

$$(p_z w)^2 = (t - p_x u - p_y v)^2. \quad (9)$$

Equating the right hand sides of equations (8) and (9), the following polynomial in  $t$  is finally obtained:

$$n_4 t^4 + n_3 t^3 + n_2 t^2 + n_1 t + n_0 = 0, \quad (10)$$

where

$$\begin{aligned} n_4 &= -\frac{(C_4 C_3 - C_2 C_5)^2}{C_1^4}, \\ n_3 &= -\frac{2}{C_1^4}(C_1^2(C_5 C_3 + C_4 C_2) \\ &+ C_1(C_5^2 + C_4^2)(C_2 x_1 + (C_1 + C_4 x_1 + C_5 y_1)z_1 + y_1 C_3) \\ &+ (C_4 C_3 - C_5 C_2)(E_5 C_2 + E_2 C_5 - E_4 C_3 - E_3 C_4)). \end{aligned} \quad (11)$$

and  $n_2$ ,  $n_1$  and  $n_0$  depend also on constant parameters, but are not provided for space reasons.

Each of the four roots of (10) determines a single value for  $p_x$ ,  $p_y$ ,  $u$ , and  $v$  through (7) and two sets of values for  $p_z$  and  $w$  by simultaneously solving  $\|\mathbf{i}\| = 1$  and  $t = \mathbf{p} \cdot \mathbf{i}$ . Thus, up to 8 assembly modes are obtained for a given set of leg lengths.

The polynomial in equation (10) is the maximum degree polynomial that we have to solve to obtain the forward kinematics solutions, so we say that the general solution for the 5-S $\underline{\text{P}}\underline{\text{U}}$  manipulator with planar base and linear platform is *quartic*.

### III. SINGULARITY-INVARIANT LEG REARRANGEMENTS

Now we want to explore possible changes of leg attachments in both the planar base  $\Pi$  and the linear platform  $\Lambda$  that leave the robot's singularity locus invariant. To this aim, we first interpret the singularity equation (2) as an unfolding of a surface in the 3D space of leg attachments, whose simple characterization in terms of a distinguished point (denoted  $\mathcal{B}$  in what follows) and a single line through it (denoted  $\mathcal{B}_\infty$ ) permits deriving geometric rules to perform the sought singularity-invariant leg rearrangements.

### A. Algebraic Formulation

Consider the following 2D surface in  $\mathbb{R}^3$

$$\begin{vmatrix} z & x & y & xz & yz & 1 \\ z_1 & x_1 & y_1 & x_1z_1 & y_1z_1 & 1 \\ z_2 & x_2 & y_2 & x_2z_2 & y_2z_2 & 1 \\ z_3 & x_3 & y_3 & x_3z_3 & y_3z_3 & 1 \\ z_4 & x_4 & y_4 & x_4z_4 & y_4z_4 & 1 \\ z_5 & x_5 & y_5 & x_5z_5 & y_5z_5 & 1 \end{vmatrix} = 0, \quad (12)$$

which can be interpreted as the hypersurface defined by points  $(x_i, y_i, z_i), i = 1, \dots, 5$ , in the 3D space of leg attachments introduced in the preceding section. The Laplace expansion by the elements of the first row of such determinant leads to the equation

$$C_1z + C_2x + C_3y + C_4xz + C_5yz + C_6 = 0, \quad (13)$$

where  $C_i$  are the cofactors of the elements of the first row, for  $i = 1, \dots, 5$ . Note that these are the same coefficients as those in the singularity polynomial (2). If any leg is substituted by a new one going from the base attachment  $\mathbf{a} = (x, y, 0)$  to the platform attachment  $\mathbf{b} = \mathbf{p} + z\mathbf{i}$ , for any  $(x, y, z)$  satisfying (13), the values of the coefficients  $C_i$  for  $i = 1, \dots, 6$  will remain the same up to a constant multiple. Hence the points with the coordinates of the five leg attachments belong to the surface defined by (13), and we can freely move them within this surface without altering the platform's singularity locus. This is because the coefficients of the singularity polynomial in (2) remain the same up to a scalar multiple and, as a consequence, its root locus remains invariant. The only caution required is that this scalar multiple be different from zero, as otherwise the platform would be architecturally singular. It is worth noting that, in this case, the coordinates of the resulting five legs would not define a surface in implicit form through equation (12).

### B. Geometric Rules to Perform Leg Rearrangements

We like to study what leg rearrangements leave the surface defined by (13) unchanged, and thus keep the platform singularity locus invariant. To this aim, let us rewrite equation (13) in matrix form as

$$[(C_2 \ C_3 \ C_6) + z(C_4 \ C_5 \ C_1)] \begin{pmatrix} x \\ y \\ 1 \end{pmatrix} = 0. \quad (14)$$

For each pair  $(x, y)$ , there is a unique corresponding  $z$  through (14), provided  $(C_4x + C_5y + C_1) \neq 0$ . Conversely, for each value of  $z$ , equation (14) defines a unique line in variables  $x$  and  $y$ . This also holds for  $z = \infty$ , whose corresponding line is:

$$\{(x, y) \mid C_4x + C_5y + C_1 = 0\}. \quad (15)$$

Equation (14) has the form of a projective pencil of lines, where each line of the pencil is formed by a linear combination of the line (15) and the line  $C_2x + C_3y + C_6 = 0$ . Then, the vertex of the pencil is the point that belong to both lines, i.e.,

$$\mathcal{B} = \left( \frac{C_3C_1 - C_6C_5}{C_2C_5 - C_4C_3}, -\frac{C_2C_1 - C_4C_6}{C_2C_5 - C_4C_3} \right), \quad (16)$$

for which any value of  $z$  satisfies equation (14).

Figure 3 shows that the surface defined by (13) has the shape of a spiral-like ruled surface around a vertical axis passing through point  $\mathcal{B}$  (16) in the  $xy$ -plane, and approaching a line parallel to (15) as  $z$  tends to  $\infty$ . This can be recognized as a hyperbolic paraboloid with two directing lines at infinity, which are obtained by intersecting the planes  $z = 0$  and  $C_4x + C_5y + C_1 = 0$  with the plane at infinity.

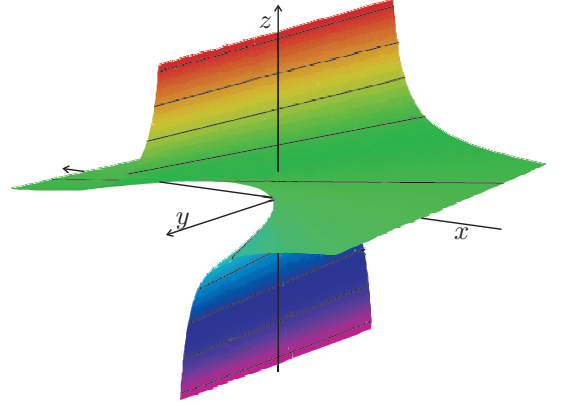


Fig. 3. Representation of surface (13) with the origin placed at point (16), and the  $y$ -axis placed at line (15).

Interpreting this surface in the 3D space of leg attachments—where  $(x, y)$  and  $z$  are the coordinates of the attachments in the base plane  $\Pi$  and the platform line  $\Lambda$ , respectively—we note that equation (14) defines a one-to-one correspondence between points in  $\Lambda$  and lines of a pencil in  $\Pi$ , with vertex at  $\mathcal{B}$  (see Fig. 4).

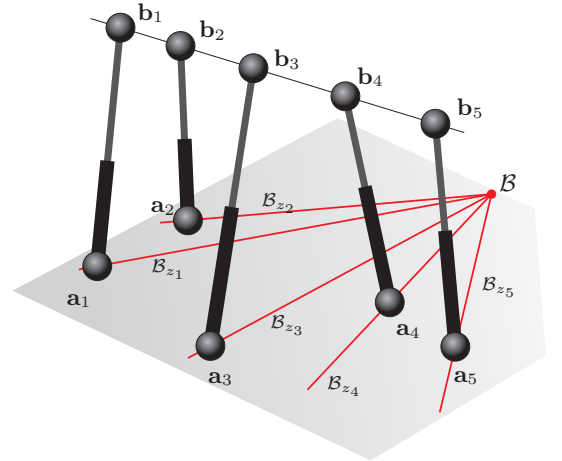


Fig. 4. The one-to-one correspondence between the attachments in the platform line and the lines of the pencil centered at  $\mathcal{B}$ . Each value of  $z_i$  defines a point in the platform line,  $\mathbf{b}_i = \mathbf{p} + z_i\mathbf{i}$ , and a line in the plane  $\mathcal{B}_{z_i}$ .

In what follows, any line in  $\Pi$  passing through point  $\mathcal{B}$  will be called a  $\mathcal{B}$ -line. The  $\mathcal{B}$ -line associated with the attachment in  $\Lambda$  with local coordinate  $z_i$  will be denoted  $\mathcal{B}_{z_i}$ . Of particular interest is  $\mathcal{B}_\infty$  given in equation (15), because in practice no attachment in  $\Pi$  can be located on it (with the exception of  $\mathcal{B}$ ), as the corresponding attachment on  $\Lambda$  should have to be moved to infinity. Moreover, the surface defined by (13) will

be called  $\mathcal{B}$ -surface when interpreted in the 3D space of leg attachments.

Summarizing, we can state two simple rules to move the leg attachments without altering the singularity locus of a given 5- $\underline{SPU}$  platform with planar base and linear platform, namely:

- for fixed platform attachments, all attachments in the base plane can be freely moved along their  $\mathcal{B}$ -lines; and
- for fixed base attachments, an attachment in the linear platform can be freely moved if, and only if, the corresponding attachment in the base is located at  $\mathcal{B}$ .

Again, the only caution required is to avoid falling into architecturally singular designs, which can be easily detected because all  $C_i$ 's,  $i = 1 \dots 6$ , would be zero. These architecturally singular designs originated by degeneracies, such as placing three attachments on the same  $\mathcal{B}$ -line or having four collinear attachments on the base, were already characterized in [18].

### C. Geometric Interpretation of Parallel Singularities

Let us rewrite (2) in vector form as:

$$[w(C_2 \ C_3 \ C_6) - p_z(C_4 \ C_5 \ C_1)] \begin{pmatrix} p_x w - p_z u \\ p_y w - p_z v \\ w \end{pmatrix} = 0. \quad (17)$$

The parallel singularities of the analyzed 5- $\underline{SPS}$  robot correspond to those configurations, defined by  $\mathbf{p} = (p_x, p_y, p_z)$  and  $\mathbf{i} = (u, v, w)$ , that satisfy the above equation. Then, two situations arise:

- If  $w \neq 0$ , (17) yields

$$[(C_2 \ C_3 \ C_6) + \mu(C_4 \ C_5 \ C_1)] \begin{pmatrix} p_x + \mu u \\ p_y + \mu v \\ 1 \end{pmatrix} = 0, \quad (18)$$

where  $\mu = -p_z/w$ . The first term of the equation defines a pencil of lines, the same pencil obtained in the previous section. Now, observe that  $\Lambda$  intersects  $\Pi$  at:

$$\mathcal{A} = (p_x + \mu u, p_y + \mu v, 0). \quad (19)$$

Then, according to (18), the singularity occurs when point  $\mathcal{A}$  lies on the line defined by  $\mathcal{B}_0 + \mu\mathcal{B}_\infty$ , that is, the line of the pencil corresponding to  $z = -p_z/w$ . Note that, if  $\mathcal{A}$  coincides with  $\mathcal{B}$ , the focus of the pencil, the manipulator would be singular for any value of  $p_z$  and  $w$ , because  $\mathcal{A}$  would simultaneously lay on all lines of the pencil.

- If  $w = 0$ , (17) yields

$$(C_4 \ C_5) \begin{pmatrix} p_z u \\ p_z v \end{pmatrix} = 0. \quad (20)$$

In this case, the manipulator is singular when  $\Lambda$  is parallel to  $\mathcal{B}_\infty$ , that is, when  $\mathbf{i} = \pm \frac{1}{\sqrt{C_4^2 + C_5^2}}(C_5, -C_4, 0)$ .

If, in addition,  $p_z = 0$ ,  $\Lambda$  necessarily lies on  $\Pi$ , which is a trivial singularity.

In sum, the 5- $\underline{SPU}$  manipulator is in a singular configuration iff the platform point  $\mathbf{p} + z\mathbf{i}$  intersecting the base does so

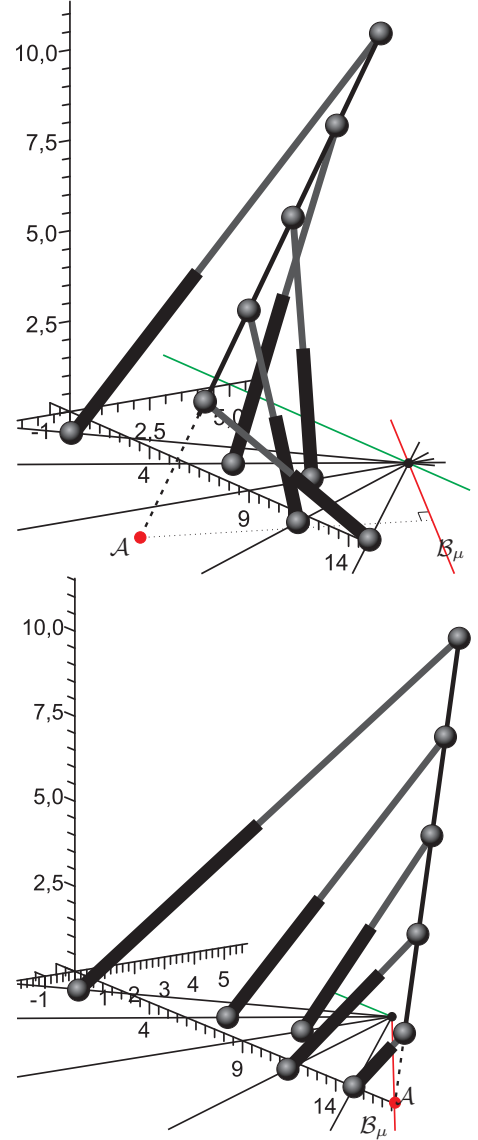


Fig. 5. A non-singular pose of the manipulator, for the position  $\mathbf{p} = (5, 8, 13)$ ,  $\mathbf{i} = (1/3, -2/3, -2/3)$  (top). A singular pose,  $\mathbf{p} = (7\sqrt{6} - 7, 4, 14)$  and  $\mathbf{i} = (\frac{\sqrt{6}}{6}, -\frac{\sqrt{6}}{6}, -\frac{\sqrt{6}}{3})$  of the manipulator (bottom).

precisely at its corresponding  $\mathcal{B}$ -line  $\mathcal{B}_z$ . Note that this includes the cases in which  $w = 0$ .

The above geometric interpretation has two very interesting implications. First, a configuration is singular iff a leg can attain zero length through a singularity-invariant leg rearrangement. The attachments of such a leg will both coincide with the point where the platform intersects the base. Second, this zero-length leg condition holding at singularities permits equating the coordinates of attachments in the base  $\mathbf{a} = (x, y, 0)^T$  and platform  $\mathbf{b} = \mathbf{p} + z\mathbf{i}$  at point  $\mathcal{A}$ , leading to the following change of variables:

$$\begin{aligned} xw &= p_x w - p_z u \\ yw &= p_y w - p_z v \\ zw &= p_z \end{aligned} \quad (21)$$

which, if applied to equation (2), yields:

$$(-w^2)(C_1 z + C_2 x + C_3 y + C_4 z x + C_5 z y + C_6) = 0. \quad (22)$$

When  $w \neq 0$ , this reduces to equation (13). Therefore, except for configurations in which the platform lies parallel to the base, the  $\mathcal{B}$ -surface (13) in the 3D space of leg attachments provides a characterization of singularities equivalent to the hypersurface equation (2) in the 5D robot configuration space.

#### D. Example I

Multiple spherical joints exist in most well-studied Gough-Stewart platforms. Such joints simplify the kinematics and singularity analysis of parallel manipulators, but they are difficult to construct and present small joint ranges, which make them of little practical interest. In this example it is shown how the presented leg rearrangements can be used to eliminate multiple spherical joints from a particular design, without losing the advantages of having simple kinematics and maintaining the same singularity locus.

Consider the 5-SPU manipulator depicted in Fig. 6(top), which is clearly of the line-plane type studied in this paper. A set of leg rearrangements can be performed to transform it into a platform with the same singularities, but with no multiple spherical joints. One of the possible sequences of leg rearrangements to attain this goal appears in Fig. 6(bottom)<sup>1</sup>.

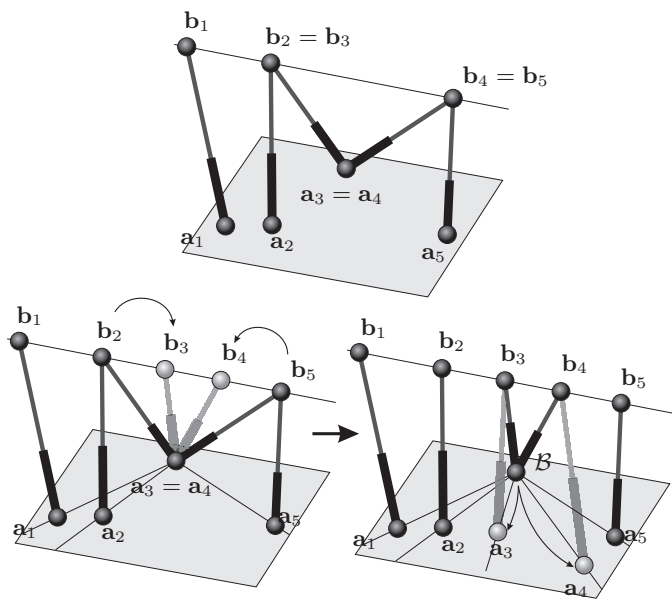


Fig. 6. Singularity-invariant leg rearrangements can be used at the manipulator design stage to eliminate multiple spherical joints.

Two remarks may ease the practical application of the leg rearrangement rules presented in the preceding section:

- There can be at most two coincident attachments on the base plane, which must lie on point  $\mathcal{B}$ . Otherwise, the manipulator either would contain a four-legged rigid component or it would be architecturally singular.
- Along a design process, the location of point  $\mathcal{B}$  may be conveniently specified by placing two coincident attachments, which can be separated later on using appropriate leg rearrangements.

<sup>1</sup>Check file 04\_The\_3-4\_5-UPS.mw in the multimedia attached archive for a numerical example.

#### E. Example II

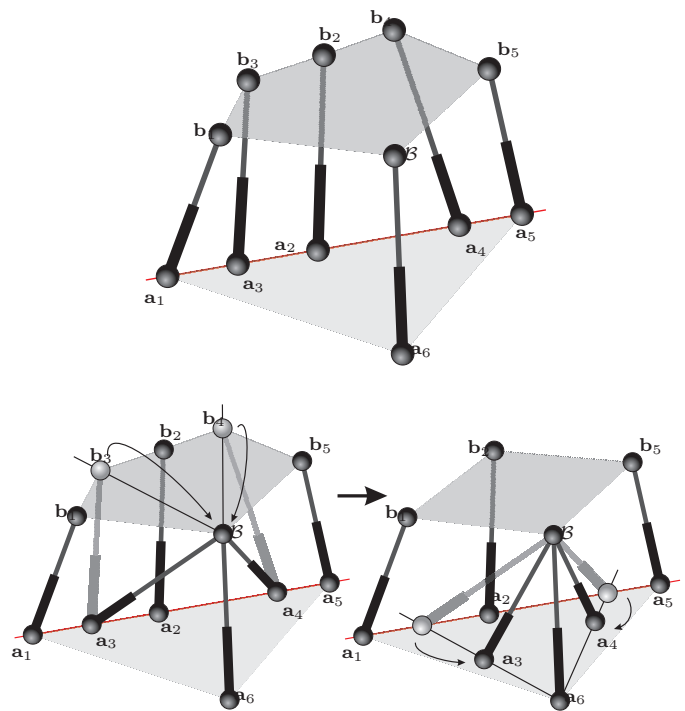


Fig. 7. From a plane-line component in the top figure, an uncoupled manipulator is obtained using singularity-invariant leg rearrangements.

Consider the Stewart-Gough platform in Fig. 7(top). It contains an upside-down line-plane component. Hence, the associated pencil of lines lies, in this case, in the platform plane. Moreover, the attachment in the platform of the leg not included in the line-plane component is made to be coincident with the focus of the pencil,  $\mathcal{B}$ .

According to the results presented in Section III-B, two platform attachments can be moved along their  $\mathcal{B}$ -lines to meet at  $\mathcal{B}$  without modifying the singularity locus of the considered platform. A point-plane component thus arises (Fig. 7(left-bottom)). It can be shown that the attachments in the plane of a point-plane component can be arbitrarily relocated, without changing the singularity locus of the whole platform, provided that no architectural singularities are introduced [27]. As a consequence, it is possible to misalign two of the base attachments (Fig. 7(right-bottom)). The result is an uncoupled parallel platform because the legs of the point-plane component determine the location of a point in the moving platform and the other three legs, the platform's orientation. It can be said that the resulting uncoupled manipulator contains a concealed line-plane component. Thus, it is clear that the presented study transcends that of 5-SPU platforms.

## IV. CLASSIFYING 5-SPU PLATFORMS BY THEIR SINGULARITIES

### A. Platform Families with Identical Singularities

Once the leg rearrangements that preserve singularity loci have been identified, we like to classify platforms in families that share each such locus. To this end, we first identify the geometric entities that fully describe the singularity locus.

It is interesting to realize that it is possible to locate a copy of  $\Lambda$  onto  $\Pi$ , parallel to the line  $\mathcal{B}_\infty$ ,

$$\Lambda^+ = \left\{ (x, y) \mid C_4x + C_5y + C_1 + \frac{C_2C_5 - C_3C_4}{\sqrt{C_4^2 + C_5^2}} = 0 \right\}, \quad (23)$$

so that each attachment in  $\Lambda^+$  lies on its associated  $\mathcal{B}$ -line in  $\Pi$  (Fig. 8).

Let us denote the coordinates of the intersections of  $\Lambda^+$  with  $\mathcal{B}_{z_i}$  by  $\mathbf{b}_i^+$ . Notice that  $\mathbf{b}_i^+$ ,  $i = 1, \dots, 5$ , are spaced at the same distances in  $\Lambda^+$  as  $\mathbf{b}_i$ ,  $i = 1, \dots, 5$ , in  $\Lambda$ . Then,  $\Lambda^+$  is a privileged line in  $\Pi$  that represents a possible location for  $\Lambda$  so that the attachments in it coincide with their corresponding  $\mathcal{B}$ -lines.

Given a particular manipulator, point  $\mathcal{B}$ , line  $\mathcal{B}_\infty$  and line  $\Lambda^+$  can be computed using (16), (15) and (23), respectively. These determine the five  $\mathcal{B}$ -lines passing through the base attachments, and their intersections with  $\Lambda^+$ ,  $\mathbf{b}_i^+$ ,  $i = 1, \dots, 5$ , determine also the location of the attachments  $\mathbf{b}_i$ ,  $i = 1, \dots, 5$  in  $\Lambda$  (see Fig. 8).

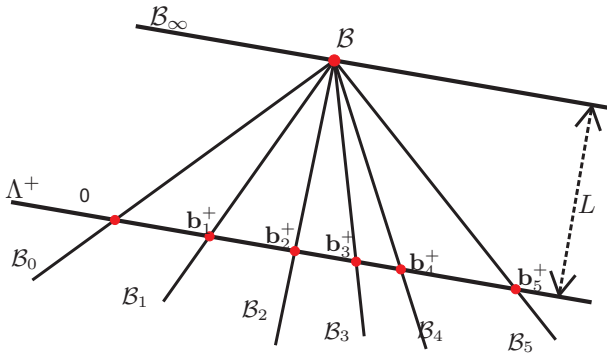


Fig. 8. Planar geometric construction that defines all the geometric parameters in a 5-SPU manipulator with planar base and linear platform.

As a consequence, point  $\mathcal{B}$ , line  $\mathcal{B}_\infty$  and line  $\Lambda^+$  characterize a family of 5-SPU manipulators having exactly the same singularity locus. Furthermore, assuming that point  $\mathcal{B}$  is finite, we can always apply a planar affine transformation that moves  $\mathcal{B}$  to the origin and line  $\mathcal{B}_\infty$  to the  $y$ -axis. Then, the  $\mathcal{B}$ -surfaces associated with two non-architecturally singular 5-SPU manipulators differ at most on a *scaling factor*, namely the distance of point  $\mathcal{B}$  to line  $\Lambda^+$  (named  $L$  in Fig. 8). This factor regulates the attachments spacing in the platform line in relation to the attachments spacing in the base plane<sup>2</sup>.

Therefore, all non-architecturally singular 5-SPU manipulators with a finite point  $\mathcal{B}$  have associated  $\mathcal{B}$ -surfaces with the same topology. Moreover, through the change of variables in (21), we can conclude that the singularity loci of all these manipulators have also the same topology.

### B. Three Possible Topologies for the Singularity Locus

So far we have assumed that point  $\mathcal{B}$  was finite. Now, suppose we take it to infinity. According to equation (16), this

<sup>2</sup>To visualize the effect of moving line  $\Lambda^+$  and point  $\mathcal{B}$  on the geometry of the manipulator, a video has been attached as a multimedia material, definingGeometricElements.avi

implies that  $C_2C_5 - C_4C_3 = 0$ . By introducing this constraint into equation (13), we obtain:

$$(C_4z + C_2)x + (C_3/C_2)(C_4z + C_2)y + C_1z + C_6 = 0. \quad (24)$$

It turns out that all  $\mathcal{B}$ -lines have now the same slope,  $C_3/C_2 = C_5/C_4$ , and, therefore, they are all parallel to  $\mathcal{B}_\infty$ . Figure 9(center) shows the corresponding  $\mathcal{B}$ -surface with the  $y$ -axis placed at line  $\mathcal{B}_\infty$ . Note, thus, that the  $\mathcal{B}$ -surface approaches asymptotically line  $\mathcal{B}_\infty$  as  $z$  tends to  $\pm\infty$ . Moreover, the  $\mathcal{B}$ -line associated with the value of  $z$  for which  $C_4z + C_2 = 0$  is the line at infinity. This appears as the surface asymptotically approaching a horizontal plane  $C_4z + C_2 = 0$  in the central graphic in Fig. 9, which can be recognized as a hyperbolic cylinder.

Thus, it is worth remarking that, in the one-to-one correspondence between points in  $\Lambda$  and lines in  $\Pi$ , we have here that a finite point in  $\Lambda$  has its associated  $\mathcal{B}$ -line at infinity, while the point at infinity in  $\Lambda$  is associated with the finite  $\mathcal{B}_\infty$  line.

Next let us explore what would happen if these two lines are made to be coincident, i.e.,  $\mathcal{B}_\infty$  is taken to infinity. Since point  $\mathcal{B} \in \mathcal{B}_\infty$ ,  $\mathcal{B}$  also stays at infinity as before. This further condition implies that  $C_4 = C_5 = 0$ , and equation (24) reduces to:

$$C_2x + C_3y + C_1z + C_6 = 0. \quad (25)$$

Of course all  $\mathcal{B}$ -lines continue to be parallel, but observe that their spacing has now become a linear function of  $z$ , namely,  $C_1z + C_6$ . Thus, the  $\mathcal{B}$ -surface is a plane in this case. Figure 9(right) shows this planar  $\mathcal{B}$ -surface with  $\mathcal{B}$ -lines parallel to the  $y$ -axis. Note that the  $\mathcal{B}$ -surface approaches line  $\mathcal{B}_\infty$  linearly as  $z$  tends to  $\pm\infty$ .

In sum, there are only three possible topologies for the  $\mathcal{B}$ -surfaces associated with non-architecturally singular 5-SPU manipulators: one when point  $\mathcal{B}$  is finite (Fig. 9(left)), another when  $\mathcal{B}$  is taken to infinity but  $\mathcal{B}_\infty$  remains finite (Fig. 9(center)), and the third when both point  $\mathcal{B}$  and line  $\mathcal{B}_\infty$  are taken to infinity (Fig. 9(right)). Again, through the change of variables in (21), we can conclude that the manipulators in each of these three families have singularity loci with the same topology.

### C. Quartic, Cubic and Quadratic cases

At the end of Section II-B we mentioned that the general solution of the forward kinematics for the 5-SPU manipulator with planar base and linear platform is *quartic*, since it entails finding the roots of polynomial (10).

Now note that, when point  $\mathcal{B}$  lies at infinity,  $C_2C_5 - C_4C_3 = 0$ , the leading coefficient  $n_4$  in equation (10) vanishes, and the forward kinematic solution becomes *cubic*. Then we only obtain 6 assembly modes for the platform line  $\Lambda$ . Finally, if not only  $\mathcal{B}$  is at infinity, but also line  $\mathcal{B}_\infty$  (that is,  $C_4 = C_5 = 0$ ), it is easy to see that also the coefficient  $n_3$  in (10) becomes zero, leading to a *quadratic* solution. When this happens, the maximum simplification of the kinematics is obtained: a platform with 4 assembly modes.

Thus, let us remark that the three topologies of the singularity locus derived in the preceding section correspond to the

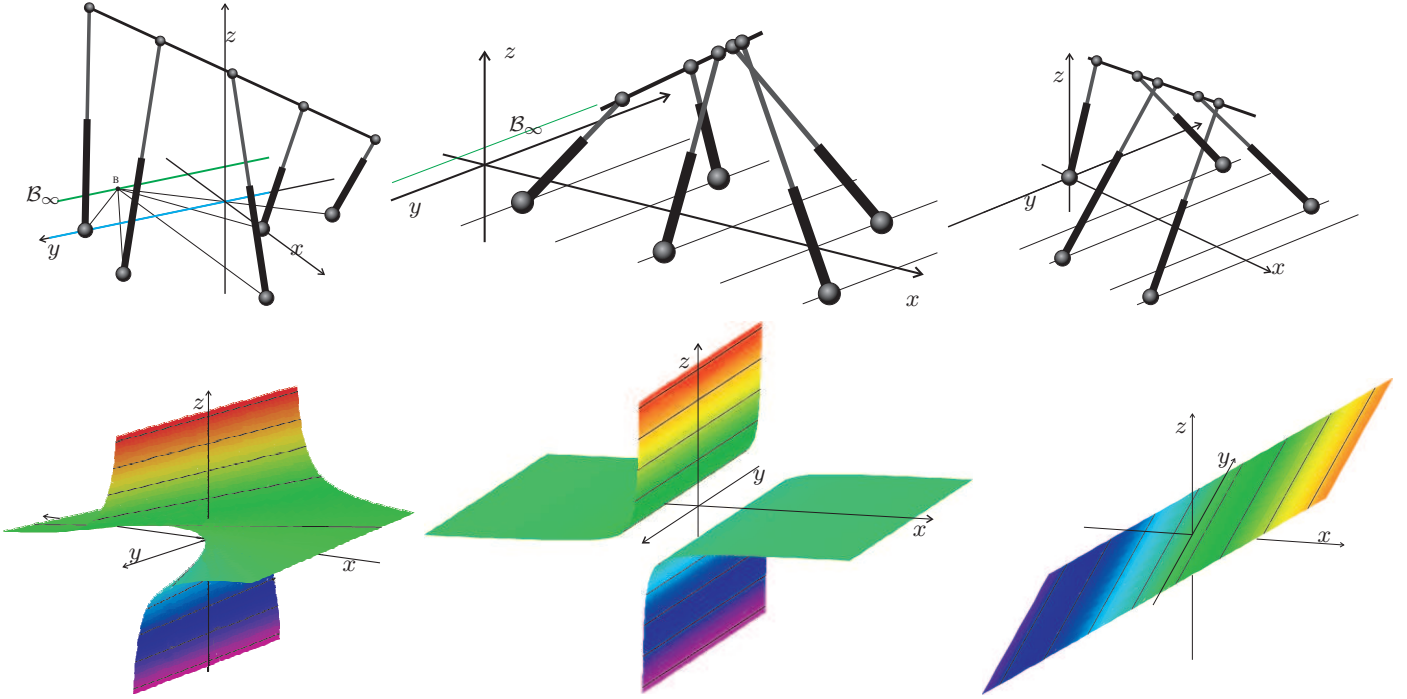


Fig. 9. Quartic, cubic and quadratically solvable 5-SPU manipulators (from top-left to top-right), with their corresponding  $\mathcal{B}$ -surfaces (bottom).

quartically-solvable 5-SPU robot family, the cubically-solvable family, and the quadratically-solvable one (Fig. 9).

#### D. Singularity hypersurface analysis

Let us briefly discuss what the slices of the singularity hypersurface for a fixed platform orientation would look like, for each topology.

For the quartic case, taking  $(u, v, w) = (0, 0, -1)$ , which corresponds to the platform line  $\Lambda$  placed perpendicular to the base plane  $\Pi$ , the 2D slice will look exactly as the  $\mathcal{B}$ -surface displayed in Fig. 3, since equation (2) reduces to (13). Thus, to every neighboring point in the sphere of platform orientations will correspond a slightly different 2D slice, and we can visualize the 4D singularity hypersurface as the combination of these spherically arranged 2D slices.

Figure 10(top) illustrates the evolution of the singularity slice when  $(u, v, w)$  moves from one pole  $(0, 0, 1)$  towards the equator  $(u, v, 0)$  of the sphere of orientations. In general, the spiral-like surface progressively flattens and, for the limiting case in which  $w = 0$ , it becomes a plane. Note that this relates to the assumption  $w \neq 0$  that we made in the change of variables (21). When  $w = 0$ , the platform line  $\Lambda$  of the manipulator is parallel to the base plane  $\Pi$ , and the equation of the singularity locus reduces to  $p_z^2(C_4u + C_5v) = 0$ . Two subcases need to be distinguished:  $p_z = 0$  and  $C_4u + C_5v = 0$ . In the former,  $\Lambda$  lies on  $\Pi$ , and the spiral surface becomes the plane  $p_x p_y$ , as mentioned. In the latter subcase, i.e., when  $C_4u + C_5v = 0$ ,  $\Lambda$  is parallel to the  $\mathcal{B}_\infty$ -line and the singularity slice at these two equator points covers the whole space  $\mathbb{R}^3$  of coordinates  $p_x, p_y, p_z$ .

In sum, the singularity locus of a 5-SPU manipulator with a finite point  $\mathcal{B}$  is a 4D hypersurface in  $S^2 \times \mathbb{R}^3$  that can be

parametrized by coordinates  $(u, v, p_x, p_y) \in S^2 \times \mathbb{R}^2$ , except at the great circle of  $S^2$  projecting to the  $\mathcal{B}_\infty$ -line, where  $p_z$  can take any value.

For the two cases with  $\mathcal{B}$  at infinity, by fixing as before  $(u, v, w) = (0, 0, -1)$ , the 2D slices obtained will look exactly as the corresponding  $\mathcal{B}$ -surfaces. Then, by making  $(u, v, w)$  sweep the sphere of platform orientations, we can visualize each of the three 4D singularity hypersurfaces as the composition of the spherically arranged 2D slices. This is done in Fig. 10(center) for the second topology (cubic case) and in Fig. 10(bottom) for the third topology (quadratic case).

## V. 5-SPU QUADRATICALLY-SOLVABLE MANIPULATOR

A 5-DoF manipulator whose forward kinematics has a quadratic solution is of interest by itself and also as a component to be included in a general 6-DoF Stewart-Gough platform. Hence we analyze it thoroughly in this section.

Let us consider a quadratically-solvable manipulator whose line  $\mathcal{B}_\infty$  coincides with the  $p_y$ -axis, and thus its  $\mathcal{B}$ -lines are parallel to this axis. This implies that we can freely fix its leg attachment coordinates  $\mathbf{a}_i = (x_i, y_i, 0)$  and  $\mathbf{b}_i = \mathbf{p} + z_i \mathbf{i}$ , with  $\mathbf{p} = (p_x, p_y, p_z)$  and  $\mathbf{i} = (u, v, w)$  as before, subject to the only constraint

$$z_i = \delta x_i, \quad (26)$$

where  $\delta$  is, thus, a proportionality factor between platform attachments and the  $x$ -coordinates of the base attachments. To ease readability of the equations, we set  $x_1 = y_1 = 0$  without losing generality. Then  $\delta, x_i$  and  $y_i, i = 2, 3, 4, 5$ , are left as parameters that characterize the family of 5-SPU robots analyzed in this section.

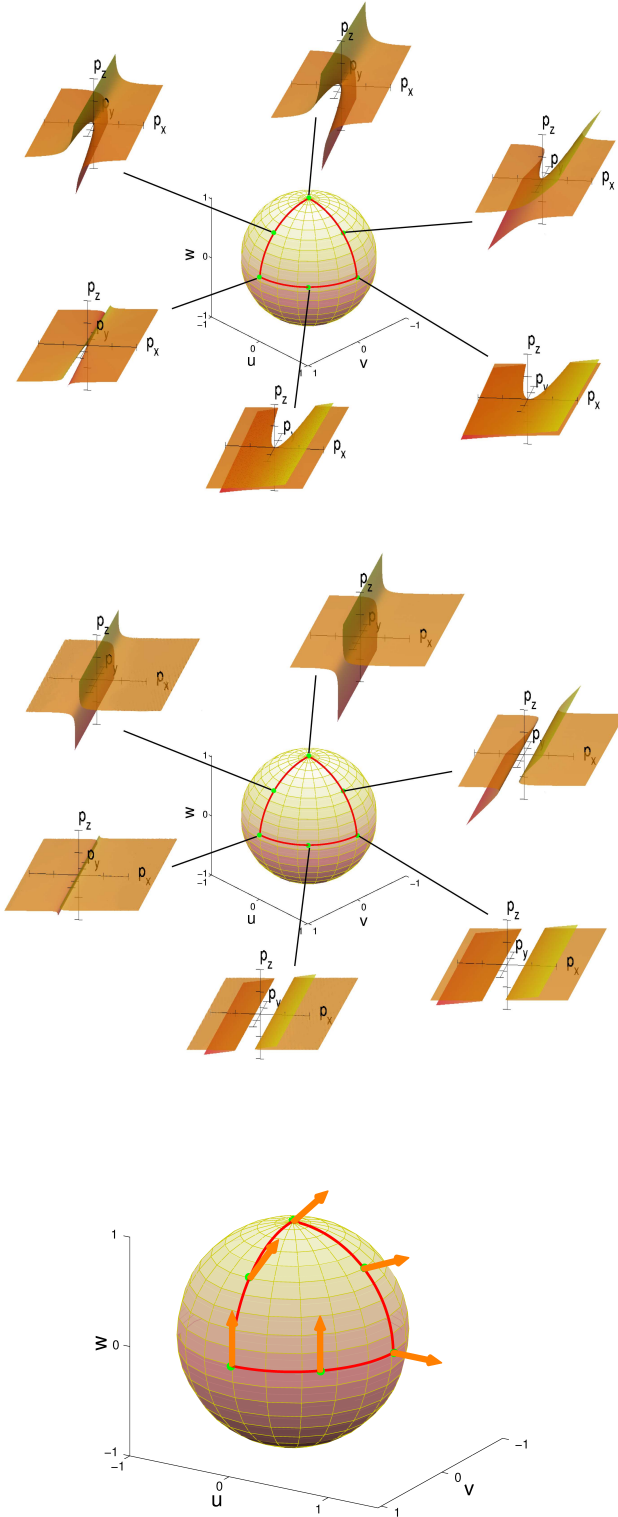


Fig. 10. Evolution of the singularity loci in the space of platform positions  $(p_x, p_y, p_z) \in \mathbb{R}^3$  as the platform orientation varies in the sphere  $(u, v, w) \in S^2$ . On top, for the case in which point  $\mathcal{B}$  is at the origin and line  $\mathcal{B}_\infty$  coincides with the  $p_y$ -axis. Center figure corresponds to the case in which point  $\mathcal{B}$  is at infinity and line  $\mathcal{B}_\infty$  coincides with the  $p_y$ -axis. Finally, in the case that line  $\mathcal{B}_\infty$  is at infinity, the slice of the singularity locus for each particular orientation is a plane. The bottom graphic displays the normal vector to this plane.

### A. Forward Kinematics

With the attachment coordinates given in (26), the cofactors of the elements of the first row of  $\mathbf{T}$  are:

$$\begin{aligned} C_1 &= \delta^2 F, \\ C_2 &= -\delta^3 F, \\ C_3 &= C_4 = C_5 = C_6 = 0, \end{aligned} \quad (27)$$

where  $F$  can be written as

$$F = \begin{vmatrix} x_2^2 & x_2 y_2 & x_2 & y_2 \\ x_3^2 & x_3 y_3 & x_3 & y_3 \\ x_4^2 & x_4 y_4 & x_4 & y_4 \\ x_5^2 & x_5 y_5 & x_5 & y_5 \end{vmatrix} \quad (28)$$

and the coefficients of polynomial (10) are:

$$\begin{aligned} n_4 &= n_3 = 0 \\ n_2 &= \frac{(\delta^2 + 1)\delta^2 F^2 - 2\delta F E_4 - E_5^2}{\delta^2 F^2} \\ n_1 &= 2 \frac{E_2 \delta^4 F^2 - F \delta (E_4 E_2 + E_5 E_3) - E_5 (E_2 E_5 - E_3 E_4)}{\delta^5 F^3} \\ n_0 &= \frac{(E_2^2 + E_3^2 + l_1^2 (E_4^2 + E_5^2)) F^2 \delta^4 - (E_2 E_5 - E_4 E_3)^2}{\delta^8 F^4} - l_1^2 \end{aligned}$$

Then, polynomial (10) becomes quadratic and, as a consequence, its two roots can be simply expressed as:

$$\begin{aligned} t &= \frac{1}{\delta^3 F (2\delta F E_4 + E_5^2 - (\delta^2 + 1)\delta^2 F^2)} \\ &\quad \left[ \delta^4 F^2 E_2 - \delta F (E_2 E_4 + E_5 E_3) \right. \\ &\quad \left. + E_5 (E_3 E_4 - E_2 E_5) \pm \sqrt{\Delta} \right], \end{aligned} \quad (29)$$

where the discriminant is

$$\begin{aligned} \Delta &= \delta F (E_5^2 + E_4^2 - \delta^4 F^2) \\ &\quad [2\delta^4 F^2 E_4 l_1^2 + \delta^3 F (E_5^2 l_1^2 + E_3^2) + \delta F (E_2^2 + E_3^2) \\ &\quad - (\delta^2 + 1)\delta^5 F^3 l_1^2 + 2E_3 (E_2 E_5 - E_4 E_3)]. \end{aligned} \quad (30)$$

Each of the two above roots, say  $t_1$  and  $t_2$ , determines a single value for  $p_x$ ,  $p_y$ ,  $u$ , and  $v$  through (7) and two sets of values for  $p_z$  and  $w$  by simultaneously solving  $\|\mathbf{i}\| = 1$  and  $t = \mathbf{p} \cdot \mathbf{i}$ . The resulting four assembly modes are explicitly given by:

$$\mathbf{p} = \begin{pmatrix} \frac{\delta^3 F t_i + E_2}{\delta^2 F} \\ \frac{E_3}{\delta^2 F} \\ \pm \frac{(E_4 - \delta F)\delta^3 F t_i + E_4 E_2 + E_5 E_3}{\delta^2 F \sqrt{\delta^4 F^2 - E_5^2 - E_4^2}} \end{pmatrix}, \quad (31)$$

and

$$\mathbf{i} = \begin{pmatrix} \frac{E_4}{\delta^2 F} \\ \frac{E_5}{\delta^2 F} \\ \pm \frac{\sqrt{\delta^4 F^2 - E_5^2 - E_4^2}}{\delta^2 F} \end{pmatrix}. \quad (32)$$

### B. Singularity Analysis

Substituting the values of the cofactors (27) into (2), the singular configurations of the studied 5-SPU platform are the solutions of the following equation

$$\delta^2 w F [\delta p_x w - (u\delta - 1)p_z] = 0. \quad (33)$$

Observe that, except for  $\delta$ , all other design parameters are embedded in  $F$ , whereas the robot pose appears only in the remaining two factors. Thus, if  $F = 0$ , the manipulator is architecturally singular, *i.e.*, it is always singular independently of its leg lengths.

Let us now turn to the case  $F \neq 0$ , and study the parallel singularities of non-architecturally singular manipulators.

A singular configuration  $(\mathbf{p}, \mathbf{i}) \in \mathbb{R}^3 \times S^2$ , with  $\mathbf{p} = (p_x, p_y, p_z)$  and  $\mathbf{i} = (u, v, w)$ , is that satisfying either  $w = 0$  or  $[\delta w p_x - (\delta u - 1)p_z] = 0$ .

Following the geometric interpretation given in Section III-C, when  $w = 0$ , the manipulator is always in a singularity, because the line  $\Lambda$  is always parallel to the  $\mathcal{B}_\infty$  (any line is parallel to a line at infinity, and for the quadratic case,  $\mathcal{B}_\infty$  is at infinity). This last condition holds for configurations where the platform is parallel to the base plane.

On the other hand, when  $w \neq 0$  equation (18) reads as

$$[(C_2 \ 0 \ 0) + \mu(0 \ 0 \ C_1)] \begin{pmatrix} p_x + \mu u \\ p_y + \mu v \\ 1 \end{pmatrix} = 0,$$

where  $\mu = \frac{-p_z}{w}$ . This condition holds when the intersection point of  $\Lambda$  with  $\Pi$ , defined as  $\mathcal{A}$  in equation (19), belongs to the line  $C_2 x + \mu C_1 = 0$ . In other words, when the point  $\mathcal{A}$  is at a distance  $\frac{p_z C_1}{w C_2} = -\frac{p_z}{w\delta}$  from the  $y$ -axis, the manipulator is in a singularity.

Note that singularities can also be expressed in joint space  $\mathbb{R}^5$  by using the discriminant (30), whose expression only depends on the leg lengths  $l_i$ ,  $i=1, \dots, 5$ . When  $\Delta = 0$  the two solutions (29) coincide, yielding a singularity. Note that  $\Delta$  also consists of two factors, the first one  $E_5^2 + E_4^2 - \delta^4 F^2 = 0$  corresponds to the condition  $w = 0$  and the other is equivalent to  $(\delta w p_x - (\delta u - 1)p_z) = 0$ .

An interesting practical consideration is that, if we fix the orientation of the tool, singularities define a plane in position space (as shown in Fig.10(bottom)):

$$c_1 p_x + c_2 p_z = 0, \quad (34)$$

with  $c_1 = \delta w^2$  and  $c_2 = w(1 - u\delta)$ . For example, if the tool is orthogonal to the base plane, *i.e.*  $(u, v, w) = (0, 0, 1)$ , then the robot will reach a singularity when its position, *i.e.*  $(p_x, p_y, p_z)$ , satisfies:

$$\delta p_x + p_z = 0. \quad (35)$$

It follows from the above singularity analysis that, for a fixed value of  $\delta$ , the whole family of non-architecturally singular 5-SPU robots considered have exactly the same singularity locus. In other words, given a member of the family, one can freely move its leg attachments without modifying the singularity locus, provided two constraints are maintained, namely the proportionality between  $x_i$  and  $z_i$ , and  $F \neq 0$  in (28) precluding architecturally singular designs.

### C. Structure of Configuration Space

The singularity locus of the 5-SPU robots studied consists of two hypersurfaces in  $\mathbb{R}^3 \times S^2$ —the robot configuration space (or C-space, for short)—, namely:

$$w = 0 \quad \text{and} \quad w p_x - \left(u - \frac{1}{\delta}\right) p_z = 0. \quad (36)$$

Note that, since  $p_y$  and  $v$  do not appear in the hypersurface equations, they do not need to be taken into account when analyzing the topology of singularities. C-space can thus be schematically represented by drawing the sphere of orientations in each point of the plane  $p_x p_z$ . Furthermore, only the projection of the sphere in the direction of the  $v$  axis needs to be displayed. Figure 11 shows such representation for eight positions around the origin in the plane  $p_x p_z$ , for the case  $\delta = 1$  (the cases  $\delta < 1$  and  $\delta > 1$  follow easily from this one, as detailed in [28]). Observe that only the relation  $p_z/p_x$  is relevant, therefore each disk stands for all positions in the half-line starting at the origin and having the same  $p_z/p_x$  value. Color encodes where the region lies in relation to the two hypersurfaces. For example, yellow points (the brightest grey level ones) are those where  $w < 0$  and  $w p_x - (u - 1/\delta)p_z < 0$ . Lines separating two colors correspond to the two hypersurfaces.

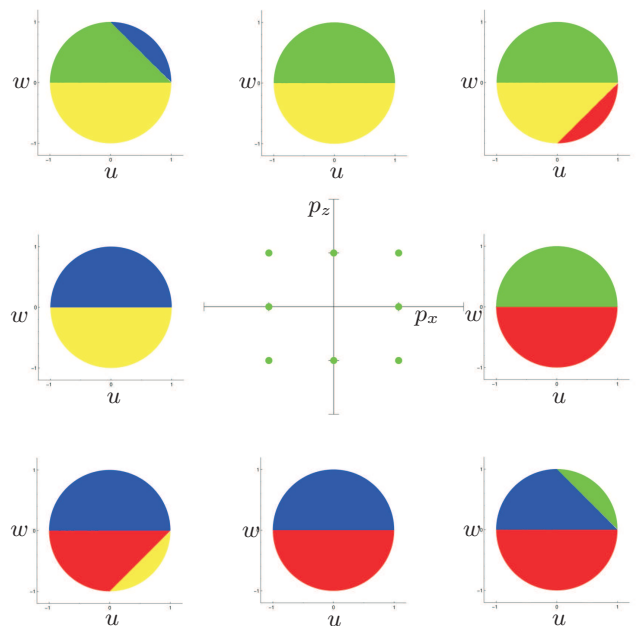


Fig. 11. Representation of the sphere of orientations for eight positions around the origin. The four connected components are marked with different colors.

Hence, the two singular hypersurfaces divide C-space into four connected components, corresponding to the four assembly modes in (31) and (32). Note that the symmetry in these equations shows up neatly in the figure. It is worth mentioning that for platform positions in the first quadrant, namely where  $p_x > 0$  and  $p_z > 0$ , all the hemisphere of orientations with  $w > 0$  is reachable. Similarly, there is a whole hemisphere reachable in the other quadrants.

Further details on the structure of C-space and its cell decomposition induced by the singularity hypersurfaces can be found in [28].

## VI. CONCLUSIONS

The complete charting of the singular configurations of individual parallel robots is important for motion planning and trajectory control. Obtaining rules to perform leg rearrangements that leave the singularity locus unchanged has a more generic interest in that it permits optimizing robot designs within a repertoire of them without having to care about collateral variations in their singularities. Even further, the establishment of entire robot families with topologically-equivalent singularity structures permits having a global view of the design options available and their associated kinematic complexities.

This paper has presented contributions at these three levels for the case of 5-SPU robots with planar base and linear platform, excluding only non-generic designs such as those with four collinear attachments in the base [26] and architecturally-singular ones. It has been shown that there are only three families with distinct topologies for the singularity locus, corresponding to quartically-, cubically- and quadratically-solvable robot platforms.

The presented analysis of 5-SPU robots is also useful for the study of 6-UPS Stewart-Gough platforms that contain a line-plane component, as it has been shown for the decoupled manipulator with three collinear attachments in Section III-E. If such component is of the quadratically-solvable type, the kinematics of the 6-DoF platform becomes greatly simplified, having a total of 8 assembly modes. A cell decomposition of its singularity locus can be readily derived from that obtained in Section V-C, by just considering the additional singular hypersurface corresponding to the platform attachment of the 6th leg lying on the base plane.

## VII. ACKNOWLEDGEMENT

The authors thank Patrick Grosch and Albert Sierra for their work on the figures, which led to fruitful discussions.

## REFERENCES

- [1] J.-P. Merlet, *Parallel Robots*. Springer, 2000.
- [2] B. Dasgupta and T. Mruthyunjayab, "The Stewart platform manipulator: a review," *Mechanism and Machine Theory*, vol. 35, pp. 15–40, 2000.
- [3] G. F. Bär and G. Weiß, "Kinematic analysis of a pentapod robot," *Journal for Geometry and Graphics*, vol. 10, no. 2, pp. 173–182, 2006.
- [4] R. Neugebauer, M. Schwaar, S. Ihlenfeldt, G. Pritschow, C. Eppler, and T. Garber, "New approaches to machine structures to overcome the limits of classical parallel structures," *CIRP Annals - Manufacturing Technology*, vol. 51, no. 1, pp. 293–296, 2002.
- [5] M. Wecka and D. Staimera, "Parallel kinematic machine tools. Current state and future potentials," *CIRP Annals - Manufacturing Technology*, vol. 51, no. 2, pp. 671–683, 2002.
- [6] T. S. Zhao, J. S. Dai, and Z. Huang, "Geometric analysis of overconstrained parallel manipulators with three and four degrees of freedom," *JSME International Journal Series C, Mechanical Systems, Machine Elements and Manufacturing*, vol. 45, no. 3, pp. 730–740, 2002.
- [7] T. S. Zhao, J. S. Dai, and Z. Huang, "Geometric synthesis of spatial parallel manipulators with fewer than six degrees of freedom," *Journal of Mechanical Engineering Science*, vol. 216, no. 12, pp. 1175–1185, 2002.
- [8] J. Gao, H. Sun, and Y. Zhao, "The primary calibration research of a measuring limb in 5-UPS/PRPU parallel machine tool," in *IEEE Intl. Conf. on Intelligent Mechatronics and Automation*, 2004, pp. 304–308.
- [9] K. Zheng, J. Gao, and Y. Zhao, "Path control algorithms for a novel 5-DoF parallel machine tool," in *IEEE Intl. Conf. on Intelligent Mechatronics and Automation*, 2005, pp. 1381–1385.
- [10] Y. Zhao, Y. Hou, Y. Shi, and L. Lu, "Dynamics analysis of a 5-UPS/PRPU parallel machine tool," in *12th IFToMM World Congress*, 2007.
- [11] Y. Lu, B. Hu, and J. Xu, "Kinematics analysis and solution of active/passive forces of a 4SPS+SPR parallel machine tool," *International Journal of Advanced Manufacturing Technology*, vol. 36, no. 1-2, pp. 178–187, 2008.
- [12] Y. Lu and J. Xu, "Simulation solving/modifying velocity and acceleration of a 4UPS+SPR type parallel machine tool during normal machining of a 3D free-form surface," *International Journal of Advanced Manufacturing Technology*, vol. 42, no. 7-8, pp. 804–812, 2009.
- [13] X. Kong and C. Gosselin, "Classification of 6-SPS parallel manipulators according to their components," in *Proc. of ASME Design Engineering Technical Conferences*, 2000, pp. DETC2000/MECH-14 105.
- [14] X.-S. Gao, D. Lei, Q. Liao, and G.-F. Zhang, "Generalized Stewart-Gough platforms and their direct kinematics," *IEEE Transactions on Robotics*, vol. 21, no. 2, pp. 141–151, 2005.
- [15] C.-D. Zhang and S.-M. Song, "Forward kinematics of a class of parallel (Stewart) platforms with closed-form solutions," in *IEEE International Conference on Robotics and Automation*, 1991, pp. 2676–2681.
- [16] C.-D. Zhang and S.-M. Song, "Forward kinematics of a class of parallel (Stewart) platforms with closed-form solutions," *Journal of Robotic Systems*, vol. 9, no. 1, pp. 93–112, 1992.
- [17] M. Husty and A. Karger, "Architecture singular parallel manipulators and their self-motions," in *International Symposium on Advances in Robot Kinematics*, Eds. J. Lenarčič and M.M. Stanišić, 2000, pp. 355–364.
- [18] J. Borràs and F. Thomas, "Kinematics of the line-plane subassembly in Stewart platforms," in *IEEE International Conference on Robotics and Automation*, 2009, pp. 4094–4099.
- [19] A. Wolf and M. Shoham, "Investigation of parallel manipulators using linear complex approximation," *Journal of Mechanical Design*, vol. 125, pp. 564–572, 2003.
- [20] H. Li, C. Gosselin, M. Richard, and B. St-Onge, "Analytic form of the six-dimensional singularity locus of the general Gough-Stewart platform," *Journal of Mechanical Design*, vol. 128, no. 1, pp. 279–287, 2006.
- [21] P. Ben-Horin and M. Shoham, "Singularity condition of six degree-of-freedom three-legged parallel robots based on Grassmann-Cayley algebra," *IEEE Transactions on Robotics*, vol. 22, no. 4, pp. 577–590, 2006.
- [22] R. Di Gregorio, "Singularity-locus expression of a class of parallel mechanisms," *Robotica*, vol. 20, pp. 323–328, 2002.
- [23] R. Di Gregorio, "Singularity locus of 6-4 fully-parallel manipulators," in *International Symposium on Advances in Robot Kinematics*, Eds. J. Lenarčič and M. M. Stanišić, 2010, pp. 437–445.
- [24] D. Downing, A. Samuel, and K. Hunt, "Identification of the special configurations of the octahedral manipulator using the pure condition," *International Journal of Robotics Research*, vol. 21, no. 2, pp. 147–159, 2002.
- [25] R. Daniel and R. Dunlop, "A geometrical interpretation of 3-3 mechanism singularities," in *International Symposium on Advances in Robot Kinematics*, Eds. J. Lenarčič and B. Roth, 2006, pp. 285–294.
- [26] J. Borràs, F. Thomas, and C. Torras, "Architecture singularities in flagged parallel manipulators," in *IEEE International Conference on Robotics and Automation*, 2008, pp. 3844–3850.
- [27] J. Borràs, F. Thomas, and C. Torras, "Singularity-invariant leg rearrangements in Stewart-Gough platforms," in *International Symposium on Advances in Robot Kinematics*, Eds. J. Lenarčič and M.M. Stanišić, 2010, pp. 421–428.
- [28] J. Borràs, F. Thomas, and C. Torras, "A family of quadratically-solvable 5-UPS parallel robots," in *IEEE International Conference on Robotics and Automation*, 2010, pp. 4703–4708.



**Júlia Borràs** received the M.Sc. degree in Mathematics in 2004 from the Technical University of Catalonia and the B.Sc. degree in Computer Science in 2006 from the Open University of Catalonia.

From 2004 to 2007 she worked in several companies as a programmer. In 2007 she joined the Institut de Robòtica i Informàtica Industrial, Barcelona, and in 2011 she received the Ph.D degree from the Technical University of Catalonia (UPC) on kinematics of parallel robots.



**Federico Thomas (M'06)** received the Telecommunications Engineering degree in 1984, and the Ph.D. degree in Computer Science in 1988, both from the Technical University of Catalonia (UPC).

He is currently Research Professor at the Spanish Scientific Research Council (CSIC), Institut de Robòtica i Informàtica Industrial, Barcelona. His current research interests are in Geometry and Kinematics with applications to Robotics, Computer Graphics and Computer Vision.

Prof. Thomas is an Associate Editor of the ASME Journal of Mechanisms and Robotics, and the International Journal of Mechanics and Control.



**Carme Torras (M'07, SM'11)** is Research Professor at the Spanish Scientific Research Council (CSIC). She received M.Sc. degrees in Mathematics and Computer Science from the Universitat de Barcelona and the University of Massachusetts, Amherst, respectively, and a Ph.D. degree in Computer Science from the Technical University of Catalonia (UPC). Prof. Torras has published five books and about two hundred papers in the areas of robot kinematics, geometric reasoning, computer vision, and neurocomputing. She has been local project leader

of several European projects, such as "Planning Robot Motion" (PROMotion), "Robot Control based on Neural Network Systems" (CONNY), "Self-organization and Analogical Modelling using Subsymbolic Computing" (SUBSYM), "Behavioural Learning: Sensing and Acting" (B-LEARN), "Perception, Action and COgnition through Learning of Object-Action Complexes" (PACO-PLUS), and the ongoing 7th framework projects "GARdeNing with a Cognitive System" (GARNICS) and "Intelligent observation and execution of Actions and manipulations" (IntellAct).

Prof. Torras is an Associate Editor of the IEEE Transactions on Robotics.